Retinal microglia initiate neuroinflammation in ocular autoimmunity

Yoko Okunuki[a], Ryo Mukai[a], Takeshi Nakao[b], Steven J. Tabor[a], Oleg Butovsky[c,d,e], Reza Dana[b], Bruce R. Ksander[b], and Kip M. Connor[a,1]

[a]Angiogenesis Laboratory, Department of Ophthalmology, Massachusetts Eye and Ear Infirmary, Harvard Medical School, Boston, MA 02114; [b]Schepens Eye Research Institute, Department of Ophthalmology, Massachusetts Eye and Ear Infirmary, Harvard Medical School, Boston, MA 02114; [c]Ann Romney Center for Neurologic Diseases, Brigham and Women's Hospital, Harvard Medical School, Boston, MA 02115; [d]Department of Neurology, Brigham and Women's Hospital, Harvard Medical School, Boston, MA 02115; and [e]Evergrande Center for Immunologic Diseases, Brigham and Women's Hospital, Harvard Medical School, Boston, MA 02115

Edited by Gabriel A. Rabinovich, University of Buenos Aires, Buenos Aires, Argentina, and approved March 26, 2019 (received for review December 3, 2018)

Autoimmune uveitis is a sight-threatening ocular inflammatory condition in which the retina and uveal tissues become a target of autoreactive immune cells. While microglia have been studied extensively in autoimmune uveitis, their exact function remains uncertain. The objective of the current study was to determine whether resident microglia are necessary and sufficient to initiate and amplify retinal inflammation in autoimmune uveitis. In this study, we clearly demonstrate that microglia are essential for initiating infiltration of immune cells utilizing a murine model of experimental autoimmune uveoretinitis (EAU) and the recently identified microglia-specific marker P2ry12. Initiating disease is the primary function of microglia in EAU, since eliminating microglia during the later stages of EAU had little effect, indicating that the function of circulating leukocytes is to amplify and sustain destructive inflammation once microglia have triggered disease. In the absence of microglia, uveitis does not develop, since leukocytes cannot gain entry through the blood-retinal barrier, illustrating that microglia play a critical role in regulating infiltration of inflammatory cells into the retina.

microglia | autoimmune uveitis | retina | blood-retinal barrier | systemic leukocytes

Autoimmune uveitis, which occurs in a variety of diseases, including Bechet's disease, sarcoidosis, and Vogt–Koyanagi–Harada disease, among many others, is a sight-threatening ocular inflammatory disease (1, 2). Although autoimmune uveitis covers a range of different clinical entities, autoimmunity against the retina and the uveal tissues is thought to be fundamental to its pathogenesis (3). Experimental autoimmune uveitis (EAU) is an animal model of human autoimmune uveitis, and is widely used to delineate the pathophysiological processes of ocular autoimmunity and develop new approaches to treat patients (4). EAU is induced by immunization against retinal antigens such as interphotoreceptor retinoid-binding protein (IRBP), which is a major component of photoreceptor outer segments, thus targeting the immune response to photoreceptors, which are the primary target of autoimmunity in autoimmune uveitis (5, 6). Immunization with IRBP and additional adjuvants leads to priming of autoreactive $CD4^+$ T cells in peripheral lymphoid organs and polarization into pathogenic Th1 and Th17 cells. Once activated, Th cells home to the eye and induce breakdown of the blood-retinal barrier, an ocular-specific immune barrier that protects eyes from destructive inflammation via tight junctions present between endothelial cells in the blood vessels that block circulating leukocyte extravasation into the retina (7).

Microglia are resident immune cells of the central nervous system, including the retina, and are important in homeostatic maintenance of the neuroretinal microenvironment (8). In healthy eyes, microglia typically have a highly ramified morphology, and their cell bodies are located in three layers in the inner retina: the ganglion cell layer, the inner plexiform layer, and the outer plexiform layer (9). Similar to brain microglia, retinal microglia keep the retina under surveillance by moving their processes and elicit multiple functions, including immune surveillance, synaptic pruning, and regulation of neurogenesis and axonal growth (10). Microglia become activated during various retinal disease processes, including pathological retinal angiogenesis (11), retinal detachment (9), retinal degeneration (12, 13), and autoimmune uveitis (14). Since activated microglia can be either beneficial (9) or harmful (12) to the affected tissue due to their altered functional states, including phagocytosis, antigen presentation, and production of inflammatory factors, controlling microglial function by immunomodulatory therapies under disease conditions is a major focus in the study of microglia (15, 16).

While the function of immune cell involvement in the development of autoimmune uveitis has been studied extensively, the exact function of microglia in the pathogenesis of this disease remains uncertain. In particular, it is still unclear what antigen-presenting cells (APCs) initiate and amplify destructive inflammation within the retina. There are two possible candidates: (*i*) microglia that are MHC class II^-, but become MHC class II^+ after activation; and (*ii*) circulating MHC class II^+ monocytes/macrophages that would first need to infiltrate the retina to trigger inflammation (17). Whether one or all of these APC populations are necessary to initiate and amplify retinal inflammation in autoimmune uveitis is unclear.

Significance

Autoimmune uveitis is a serious sight-threatening condition defined by an autoreactive immune response against uveal tissues and the retina. As a result, patients with uveitis often suffer serious visual loss after persistent inflammation due to immune-mediated damage in the targeted tissues. Microglia are resident immune cells in the retina, and are thought to be the key population that initiates retinal inflammation; however, the exact role for microglia in autoimmune uveitis is still unknown. Here, we demonstrate that microglia are essential for the induction of a retinal autoimmune response, as microglial ablation completely blocks disease. Our data suggest that microglia mediate autoreactive immune cell entry into the retina, and that by depleting microglia, circulating immune cells cannot gain entry into the retina.

Author contributions: Y.O. and K.M.C. designed research; Y.O., R.M., and T.N. performed research; Y.O., S.J.T., O.B., R.D., B.R.K., and K.M.C. analyzed data; and Y.O. and K.M.C. wrote the paper.

The authors declare no conflict of interest.

This article is a PNAS Direct Submission.

[1]To whom correspondence should be addressed. Email: kip_connor@meei.harvard.edu.

This article contains supporting information online at www.pnas.org/lookup/suppl/doi:10.1073/pnas.1820387116/-/DCSupplemental.

Published online April 25, 2019.

The problem in resolving this question in previous studies was that it had not been possible to specifically identify or eliminate only microglia, since the available markers, such as CD11b, Iba-1, and Cx3cr1, used to identify activated microglia are also expressed on monocytes/macrophages. However, in the present study, we utilized the recently identified microglia-specific marker P2ry12 (18) that is expressed on microglia but not macrophages. To determine the function of microglia during initiation and amplification of EAU, we used the colony-stimulating factor-1 (Csfr1) antagonist PLX5622 that was previously shown to selectively induce cell death in microglia in vivo (19–21), with minimal effects on other APC subpopulations. Results using PLX5622-induced microglial depletion were confirmed with a second microglia-specific depletion method utilizing local administration of diphtheria toxin (DTX) in *Cx3cr1*^{CreER} × B6-inducible diphtheria toxin receptor (iDTR) mice (22, 23). In each case, eliminating retinal microglia before mice were immunized against IRBP prevented the development of uveitis, and circulating primed immune cells were unable to infiltrate into the retina. Circulating monocytes/macrophages failed to replace the function of resident microglia in triggering the start of EAU. Therefore, microglia have the unique function of initiating infiltration of immune cells into the retina during development of autoimmune uveitis. This is the primary function of microglia in EAU, since eliminating microglia after mice were immunized against IRBP and disease had already started had no effect on the severity or progression of uveitis, indicating the function of monocytes/macrophages is to amplify and sustain destructive inflammation once microglia have triggered the initiation of the disease.

Results

Microglia Depletion by a Csf1r Antagonist, PLX5622, Suppresses Uveitis. To define the role of retinal microglia in EAU, we first determined if microglial depletion before EAU induction affected disease progression. To accomplish this, we utilized a Csf1r antagonist (PLX5622), which was shown previously to selectively induce cell death in microglia (19–21). PLX5622 rapidly depletes all retinal microglia within the inner and outer plexiform layers and the ganglion cell layer within 7 d of beginning treatment (Fig. 1*A* and *SI Appendix*, Fig. S1). Previously, we demonstrated that microglia undergo apoptosis with dietary PLX5622 treatment (9). Dietary chow containing PLX5622 (1,200 ppm) or a matched control diet was started 7 d before IRBP immunization to ensure complete depletion of retinal microglia in PLX5622-treated animals before induction of EAU. Clinical assessment of EAU pathology via fundus examination (7, 14, 21, and 28 d after induction) and histological assessment using H&E staining (21 d after induction) were conducted to monitor disease progression with treatment. The severity of retinal inflammation of each eye was assessed by evaluating the degree of vasculitis, immune cell infiltration, and damage in the retina and the choroid using previously defined disease severity scales that range between 0 and 4 and are noted in half-point increments (24, 25). Microglial depletion completely suppressed the development of EAU through day 21 ($n = 7$ mice per group; $P < 0.001$). Only one animal in the PLX5622-treated group developed very mild vasculitis that was not apparent until day 28, although 100% of the control animals developed EAU with vasculitis and chorioretinal infiltrates by day 21 (Fig. 1 *B* and *C*). Moreover, histological EAU evaluation of mice with and without microglial depletion on day 21 further confirmed that depletion of retinal microglia completely suppressed infiltrating inflammatory cells ($P < 0.01$; Fig. 1 *D* and *E*). Hallmarks of retinal inflammation such as photoreceptor folds, vitreous cells, and retinal granulomas, which were observed in the control animals, were absent in the PLX5622-treated animals that lack microglia. Cumulatively, these data demonstrate that eliminating microglia before IRBP immunization suppresses EAU development, indicating that microglia play a vital role in initiating EAU pathogenesis.

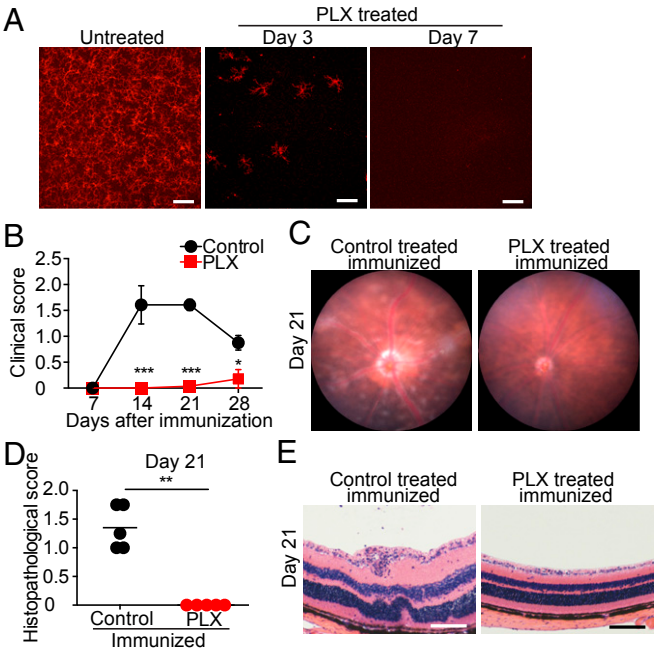

Fig. 1. Microglia depletion suppresses EAU. C57BL/6 mice were fed PLX5622 (PLX), a Csf1r antagonist, or control diet starting 7 d before IRBP immunization (day 0). (*A*) Retinas were whole-mounted and stained for P2ry12 in naive mice and mice fed PLX for 3 and 7 d. Z-stack orthogonal view images of the entire thickness (including the inner and the outer plexiform layers and the ganglion cell layer) of the midperipheral retina were taken by confocal microscopy. Representative images from three to four retinas per time point are shown. (Scale bars: 100 μm.) (*B*) Time course of EAU clinical scores ($n = 7$ mice per group) by fundus observation. Scores were graded in a blinded manner on a scale between 0 and 4 in half-point increments as described previously. Briefly, trace chorioretinal lesions and minimal vasculitis were scored as 0.5. Mild vasculitis with small focal chorioretinal lesions (≤5) were scored as 1. Severe vasculitis with multiple chorioretinal lesions (>5) were scored as 2. A pattern of a linear chorioretinal lesion, subretinal neovascularization, and hemorrhage were scored as 3. Inflammation with large retinal detachment and severe hemorrhages were scored as 4. (*C*) Representative retinal fundus images indicating a score of 1.5 in control immunized mice (vasculitis and chorioretinal lesions) but absent in PLX-treated mice on day 21. (*D*) Histopathological EAU score on day 21 ($n = 5$ mice per group) were graded in a blinded manner on a scale between 0 and 4 in half-point increments as described previously. Briefly, focal nongranulomatous, monocytic infiltration in the choroid, ciliary body, and retina were scored as 0.5. Retinal perivascular infiltration and monocytic infiltration in the vitreous were scored as 1. Granuloma formation in the uvea and retina together with the presence of occluded retinal vasculitis, photoreceptor folds, serous retinal detachment, and loss of photoreceptors, were scored as 2. In addition, the formation of granulomas at the level of the retinal pigment epithelium and the development of subretinal neovascularization were scored as 3 and 4 according to the number and the size of the lesions. (*E*) Representative histopathological (H&E staining) images indicating a score of 1.5 (photoreceptor folds, vitreous cells, and retinal granulomas) in control mice and 0 (no inflammation) in PLX-treated mice. The average of scores from both eyes was determined as the score of the animal. (Scale bars: 100 μm.) (*B* and *D*) Mann–Whitney *U* test. Data are expressed as mean ± SEM. $^*P < 0.05$; $^{**}P < 0.01$; $^{***}P < 0.001$.

Csf1r Antagonism Does Not Significantly Decrease IRBP-Specific Immune Response. Our data and prior findings from other laboratories clearly demonstrate that retinal microglia require Csf1r for survival (26). However, Csf1r is also expressed on systemic macrophages/monocytes, and we therefore could not exclude the possibility that PLX5622 treatment inhibits EAU not via eliminating retinal microglia, but by blocking the systemic induction of autoreactive immune cells. Even though previous studies indicated PLX5622 treatment has only minimal effects on circulating systemic immune cells (9, 20, 21), we nevertheless sought to evaluate

the effects of PLX5622 treatment on the development of IRBP-specific immunity via examining: (*i*) IRBP-specific delayed hypersensitivity in vivo, and (*ii*) IRBP-specific and nonspecific (Con A-induced) lymphocyte proliferation in vitro. Groups of mice analyzed were as follows: (*i*) negative controls (naive unimmunized mice), (*ii*) positive controls (control feed-treated immunized mice), and (*iii*) PLX5622-fed (microglia-depleted) immunized mice. We found that mice receiving PLX5622 treatment still generated a systemic IRBP-specific immune response, even though they failed to develop EAU. The induction of delayed hypersensitivity in the ear against IRBP-peptide 1–20 (IRBP-p) was not significantly reduced by PLX5622 treatment (Fig. 2*A*). Moreover, PLX5622 treatment did not significantly affect IRBP-specific in vitro lymphocyte proliferation using draining lymph node (LN) cells or spleen cells recovered at 14 and 21 d postimmunization (Fig. 2 *B*–*E*). There was also no evidence that PLX5622 treatment resulted in significant atrophy of lymphoid organs (Fig. 2 *F* and *G*). Together, these data indicate that while PLX5622 treatment depletes retinal microglia and suppresses development of EAU, it does not significantly inhibit the systemic induction of IRPB-reactive immune cells.

To further confirm that PLX5622 treatment did not alter the ability of mice to generate an IRBP-specific immune response, we examined the induction of $CD4^+$ T cell subpopulations that represent either effector T cells (IFN-γ– or IL-17–producing cells) or $CD4^+CD25^+Foxp3^+$ regulatory T cells. Dendritic cells ($CD11c^+CD11b^+$) and macrophages ($CD11c^{low}CD11b^+$) within the LNs and spleen were compared as frequencies among $CD45^+$ cells, a pan-leukocyte marker. We found that within the LNs and spleens of PLX5622-treated mice at 14 d postimmunization, there was a reduction in the frequency of $CD11c^+CD11b^+$ dendritic cells, a cell population that is essential for activating $CD4^+$ T cells in EAU (27, 28), but there was no significant reduction in the frequency of $CD11c^{low}CD11b^+$ macrophages (Fig. 3 *A* and *D*). By contrast, PLX5622 treatment did not significantly reduce the frequency of $CD3^+CD4^+$ T cells positive for IFN-γ^+ or IL-17^+, which are two major pathogenic cytokines in EAU (29) (Fig. 3 *B* and *E*). In addition, PLX5622 treatment did not increase the frequency of regulatory T cells, which are known to suppress EAU (30) (Fig. 3 *C* and *F*). These data demonstrate that although PLX5622 treatment caused a reduction in the frequency of dendritic cells, this reduction did not significantly reduce the ability to induce IRBP-specific cytokine-producing $CD4^+$ T cells involved in EAU. Together, these in vivo and in vitro studies indicate that PLX5622 treatment does not significantly decrease the ability of mice to induce an IRBP-specific autoimmune response, but rather disrupts immune cell infiltration.

Csf1r Antagonism Has No Effect on Uveitogenic Cell Activation in EAU. PLX5622-treated, IRBP-immunized mice that lacked retinal microglia failed to develop EAU (Fig. 1). To conclusively prove the absence of EAU in PLX5622-treated mice was due to the absence of microglia and not due to a failure to generate IRBP-reactive immune cells, we utilized the adoptive transfer model of EAU. In this model, IRBP-reactive immune cells are transferred from donor IRBP-immunized mice into naive recipient mice by i.p. injection, which subsequently develop EAU without receiving systemic immunization (31, 32). Thus, by transferring IRBP-reactive immune cells from a donor into recipient PLX5622-treated mice that lack retinal microglia, we are able to assess the contribution of microglia on the development of EAU in mice that are known to possess circulating autoreactive immune cells. This approach excludes any potential negative effects of Csf1r antagonism on the systemic cell priming stage.

When primed cells from IRBP-immunized donor mice with EAU were adoptively i.p. transferred into naive recipient mice fed the control diet, significant inflammation characteristic of EAU was induced, including severe vasculitis, optic disk swelling,

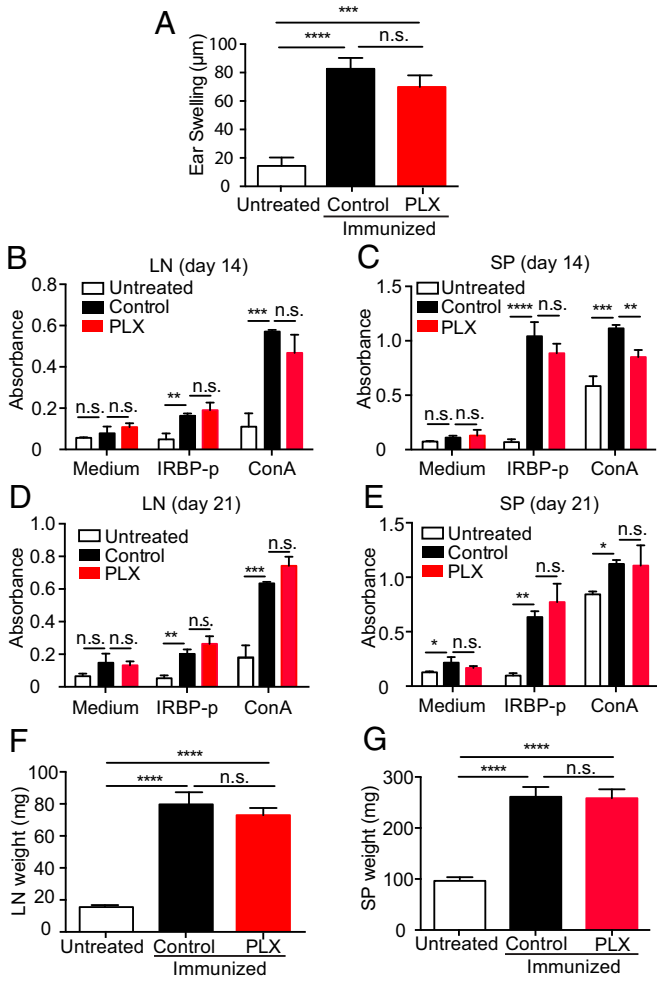

Fig. 2. Microglia depletion by a Csf1r antagonist in EAU does not alter the systemic immune response to the immunized peptide. C57BL/6 mice were fed the Csf1r antagonist PLX5622 (PLX) or a control diet 7 d before IRBP immunization, and animals were immunized on day 0. (*A*–*E*) Animals were evaluated for a systemic immune response against the IRBP-p. (*A*) Delayed hypersensitivity, as determined by ear swelling, was evaluated on day 21. Mice were injected intradermally with IRBP-p into the pinna of one ear on day 19. Ear swelling was measured after 48 h using a micrometer (n = 6–7 mice per group). (*B*–*E*) Cell proliferation was evaluated by using the cells isolated from LNs and spleens (SPs) on days 14 and 21. The cells were cultured in triplicate for 3 d in the presence of IRBP-p (10 μg), Con A (1 μg), or medium only (n = 5 mice per group). During the last 4 h before the 72-h endpoint culture, the Cell Counting Kit-8 was added to each well. At 72 h, viable cell numbers in each well were measured as the absorbance (450 nm) of reduced WST-8. (*F* and *G*) Weights of the draining LNs (n = 5 mice per group) and SPs (n = 5 mice per group) were measured on day 21. Data were analyzed by one-way ANOVA, followed by Tukey's multiple comparison test. Data are expressed as mean ± SEM. $^*P < 0.05$; $^{**}P < 0.01$; $^{***}P < 0.001$; $^{****}P < 0.0001$. n.s., not significant.

chorioretinal infiltrates, presence of vitreous cells, photoreceptor loss, and retinal folds (Fig. 4 *A*–*C*), indicating the transferred cells were capable of triggering EAU. By contrast, when these same primed cells from IRBP-immunized donor mice were transferred into naive recipient PLX5622-treated mice that lacked retinal microglia, no significant inflammation was detected, indicating the circulating primed cells were not capable of infiltrating the retina and triggering EAU when retinal microglia were not present (Fig. 4 *A*–*C*).

In addition, we used this adoptive transfer model to confirm that PLX5622 treatment did not block the induction of IRBP-reactive

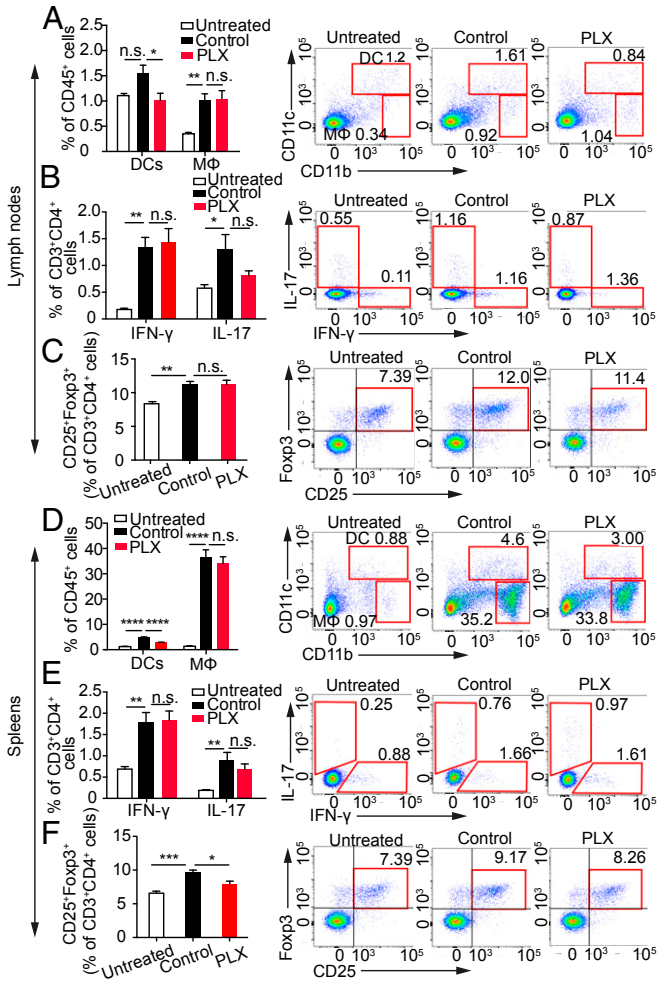

Fig. 3. Csf1r antagonism does not suppress cytokine production in cells from LNs and spleens (SPs) in EAU, but suppresses $CD11c^+CD11b^+$ dendritic cells. C57BL/6 mice fed the PLX5622 (PLX) or control diet were immunized with IRBP-p. LN cells and SP cells from immunized mice on day 14 (PLX and control) and naive mice were analyzed by flow cytometry. CD11b and CD11c expression on $CD45^+$ cells (*A* and *D*), IFN-γ and IL-17 expression on $CD3^+CD4^+$ cells (*B* and *E*), and $CD25^+Foxp3^+$ cells on $CD3^+CD4^+$ cells (*C* and *F*) in LNs (*A*–*C*) and in SPs (*D*–*F*) are shown ($n = 5$ mice per group). Data were analyzed using one-way ANOVA, followed by Tukey's multiple comparison test. Data are expressed as mean ± SEM. $^*P < 0.05$; $^{**}P < 0.01$; $^{***}P < 0.001$; $^{****}P < 0.0001$. DCs, dendritic cells; MΦ, macrophage; n.s., not significant.

immune cells capable of mediating EAU. When donor cells from mice that received PLX5622 treatment starting 7 d before IRBP immunization (−17 d) were transferred i.p. into naive recipient mice, significant inflammation characteristic of EAU was induced. Moreover, the kinetics and magnitude of the inflammation induced by these adoptively transferred cells were not significantly different from the inflammation observed in control recipient mice that received donor cells from mice not treated with PLX5622 (Fig. 4 *D* and *E*). Together, these results indicate that PLX5622 treatment does not inhibit the induction of IRBP-reactive immune cells capable of mediating EAU, and that the failure of PLX5622-treated mice to develop EAU was due to the loss of retinal microglia.

Local Ablation of $CX3CR1^+$ Retinal Microglia Suppresses EAU. To rigorously confirm the function of microglia in the development of EAU, we used a second method to deplete retinal microglia that was not dependent on blocking Csf1r. We depleted retinal microglia utilizing a transgenic mouse approach. *Cx3cr1*^{CreER} mice with a tamoxifen-inducible Cre recombinase gene controlled by the *Cx3cr1* promoter were crossed to B6-iDTR mice with a floxed DTR gene. When the resulting mice (*Cx3cr1*^{CreER} × B6-iDTR) receive tamoxifen, DTR is expressed only on CX3CR1-expressing cells, which can then be eliminated selectively by administering DTX. Approximately 90% elimination of retinal microglia can be achieved when the animals are treated with five consecutive days of systemic i.p. injections of tamoxifen followed by anterior chamber injection of DTX (9). However, tamoxifen has a known immunosuppressive effect on autoimmunity (33, 34), and this systemic tamoxifen treatment regimen, with no

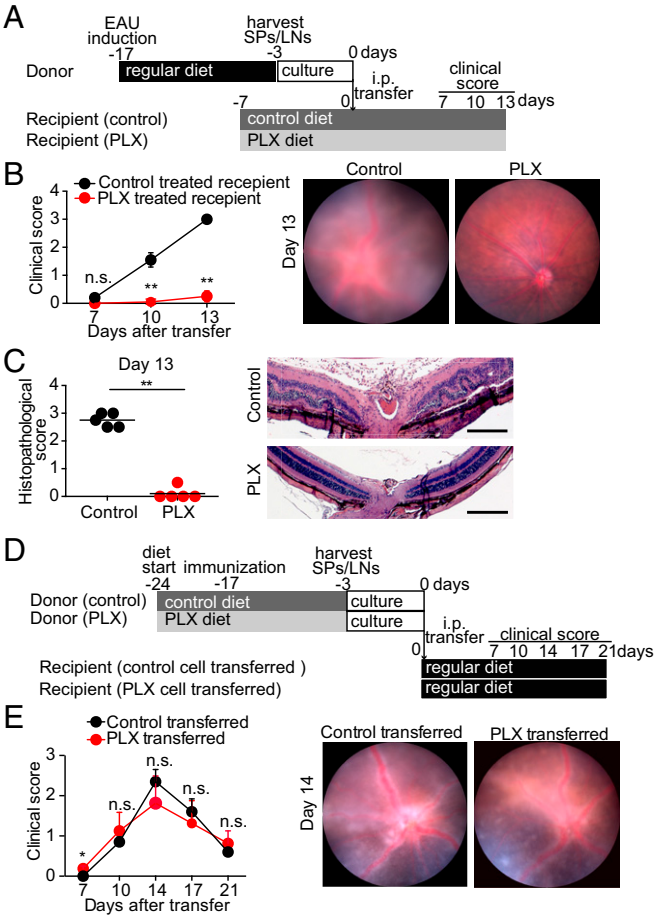

Fig. 4. Csf1r antagonism suppresses EAU in recipient mice but does not significantly suppress uveitogenicity of donor lymphocytes in adoptive transfer EAU models. Adoptive transfer EAU was induced in recipient mice by transferring activated lymphocytes from donor mice. The donor mice were immunized with IRBP-p, and spleens (SPs) and LNs were harvested 14 d postimmunization. The SP and LN cells isolated from donor mice were cultured for 3 d under stimulation with IRBP-p and IL-23. Adoptive transfer EAU was induced in recipient mice by i.p. transferring activated lymphocytes from donor mice. (*A*–*C*) PLX5622 (PLX) or control diet was given to recipient mice 7 d before cell transfer from donor mice. (*A*) Schematic time course of the experiment in which PLX was administered to recipient mice. (*B*) Time course clinical score (evaluated as in Fig. 1) and representative fundus images on day 13 ($n = 5$ mice per group). (*C*) Histopathological score on day 13 (evaluated as in Fig. 1) and representative images of the recipient PLX experiment ($n = 5$ mice per group). (*D* and *E*) PLX or control diet was given to donor mice 7 d before IRBP immunization, and cells were then i.p. transferred to recipient mice treated with a regular diet. (*D*) Schematic time course of the experiment in which PLX was given to donor mice. (*E*) Time course of clinical score and representative fundus images on day 14 in the donor PLX experiment ($n = 5$ mice per group). Mann–Whitney *U* test. Data are expressed as mean ± SEM. $^*P < 0.05$; $^{**}P < 0.01$. (Scale bars: 200 μm.)

DTX administered, suppressed development of EAU (*SI Appendix*, Fig. S2 *A* and *B*). For this reason, we administered tamoxifen locally via eye drops (22), which did not significantly reduce EAU (*SI Appendix*, Fig. S2 *A* and *C*).

Cre recombinase was activated by tamoxifen administration via eye drops (three times per day) for five consecutive days. DTX was administered via anterior chamber injections (22, 23). Using this approach, 60% of retinal microglia were depleted 48 h after DTX injection (*SI Appendix*, Fig. S3*A*). The maximum depletion of microglia via this technique was most likely limited by the amount of Cre recombinase activated by administering tamoxifen via eye drops. The adoptive transfer of the EAU method, as described above, was used to evaluate microglia depletion via this method. IRBP-reactive immune cells were generated by immunizing donor mice with IRBP. Recipient naive mice received tamoxifen treatment starting 2 wk before the adoptive transfer of donor cells. Recipient mice received anterior chamber injections of either saline (negative control) or DTX every 2 d starting 1 d before transfer of donor cells. The mice were evaluated by clinical fundus examination and histological examination on day 10 after cell transfer (*SI Appendix*, Fig. S3*B*). EAU was significantly inhibited in microglia-depleted mice but not in control mice (*SI Appendix*, Fig. S3 *C* and *D*). This confirmed that microglia direct the amount of infiltration and retinal destruction in autoimmune uveitis. EAU inhibition in these experiments was not as complete as we observed in PLX5622-treated mice, which is likely due to the degree of microglia depletion using these two techniques (60% versus 100% depletion in DTX-treated and PLX5622-treated mice, respectively).

Suppression of EAU Through Microglial Depletion Is Time-Dependent. To determine whether microglia, in addition to initiating EAU, are required to amplify and sustain retinal inflammation, we depleted microglia at various time points before and after infiltration of immune cells into the retina. In this EAU model, retinal inflammation is not observed on day 7 after immunization, and begins around day 10, indicating that autoimmune cells first infiltrate the retina between days 7 and 10 (Fig. 5*A*). In addition, PLX5622 treatment requires 7 d to eliminate retinal microglia. Therefore, to eliminate microglia after IRBP immunization but before immune cell infiltration, treatment was started on day 0 so that microglia were depleted by day 7, before immune cell infiltration and development of EAU. To eliminate microglia during the "early phase" of EAU, treatment was started on day 7 so that microglia depletion was completed by day 14, before the peak of inflammation but after immune cell recruitment. To eliminate microglia during the "late phase" of EAU, treatment was started on day 14 so that microglia depletion was completed by day 21, after the development of significant inflammation (Fig. 5*A*).

As expected, when PLX5622 treatment was started on the day of immunization (day 0), EAU was effectively suppressed (Fig. 5*B*). PLX5622-treated mice did not develop any signs of EAU postimmunization, whereas control-treated mice developed significant EAU with vasculitis and chorioretinal infiltrates. When PLX5622 treatment was started on day 7 after immunization, EAU was partially suppressed (Fig. 5*C*). PLX5622-treated mice developed very mild vasculitis around the optic disk, whereas control mice had elevated vasculitis and chorioretinal infiltrates in wide lesions. In this group, microglia were depleted by day 14, resulting in the presence of a smaller population of microglia when infiltration begins on day 10. By contrast, when PLX5622 treatment was started on day 14, the severity of EAU was not significantly different from that in control mice (Fig. 5*D*). Both PLX5622-treated and control-treated mice developed comparable inflammation with vasculitis and chorioretinal lesions. In this group, a full population of microglia is present when immune cells start to infiltrate on day 10, and complete microglial depletion would occur only during the late amplification phase. Taken together, these data indicate the primary function of microglia is to initiate inflammation in EAU, since eliminating microglia during the late phase of disease development had no effect on the severity or progression of uveitis. These data suggest the function of peripheral monocytes/macrophages is to amplify and sustain destructive inflammation once microglia have triggered the start of disease.

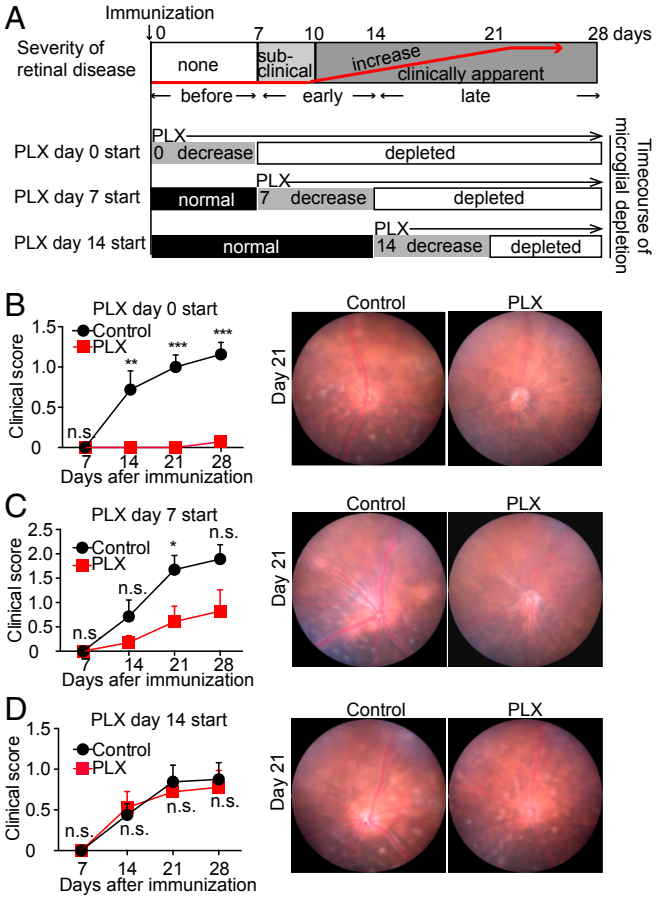

Fig. 5. Microglial depletion following IRBP immunization diminishes EAU suppression. C57BL/6 mice were immunized with IRBP, and microglia depletion by PLX5622 (PLX) was started at different time points (days 0, 7, and 14 postimmunization) so that microglia depletion started at different time points of development of EAU. The animals fed the control diet without microglia depletion served as controls. Ocular inflammation was observed every 7 d until day 28. (*A*, *Top*) Diagram illustrates a normal time course of EAU in C57BL/6 mice. (*A*, *Bottom*) Three diagrams illustrate the timing of PLX administration (days 0, 7, and 14 postimmunization) and corresponding time courses of microglial depletion. (*B*–*D*) Time course of EAU clinical inflammation (days 7, 14, 21, and 28) (evaluated as in Fig. 1) and representative fundus images on day 21. PLX or the control diet was started on day 0 (*B*), day 7 (*C*), and day 14 (*D*) after immunization [mice per group: $n = 7$–8 (*B*), $n = 7$ (*C*), $n = 8$–9 (*D*)]. Mann–Whitney *U* test. Data are expressed as mean ± SEM. $*P < 0.05$; $**P < 0.01$; $***P < 0.001$. n.s., not significant.

Microglia Interact with Adherent Vascular Leukocytes in the Early Phase of EAU. To determine the morphological stage of microglial activation during EAU, whole-mount retinas from EAU mice on days 7, 10, and 14 were stained with P2ry12 (a microglia-specific marker) and lectin (an endothelial marker for vessel staining), and then evaluated using confocal microscopy. Naive mice served as a normal control (day 0). We observed morphologically activated microglia by day 7, progressing from a highly ramified appearance into a more activated amoeboid shape as disease progressed (Fig. 6*A*, *Left* and *SI Appendix*, Fig. S4 *A* and *B*). The

number of microglia was unchanged through the early phase of EAU (*SI Appendix*, Fig. S4*C*); however, previous studies have indicated retinal microglia/macrophages migrated to the outer retina at/after the peak of EAU pathology (35, 36). Of interest, we observed that microglia remained in the retinal vascular layers (Fig. 6*A*, *Right*) and appeared to become more closely associated with retinal vessels during EAU disease progression (Fig. 6 *A*, *Center* and *B*).

Accordingly, we hypothesized that microglia may trigger recruitment of inflammatory cells via increasing adhesion of leukocytes to retinal vessels. To test this hypothesis, we examined the number of adherent leukocytes within retinal vessels during EAU in the presence or absence of microglia. We found that PLX5622-treated immunized mice that lack microglia had significantly fewer adherent cells than control-treated immunized mice (Fig. 7 *A* and *B*). Moreover, there was no significant difference in the number of adherent cells between control-treated unimmunized mice and PLX5622-treated immunized mice that lacked microglia (Fig. 7 *A* and *B*), indicating the increase in cells adhering to the retinal vasculature coincides directly with the presence of microglia.

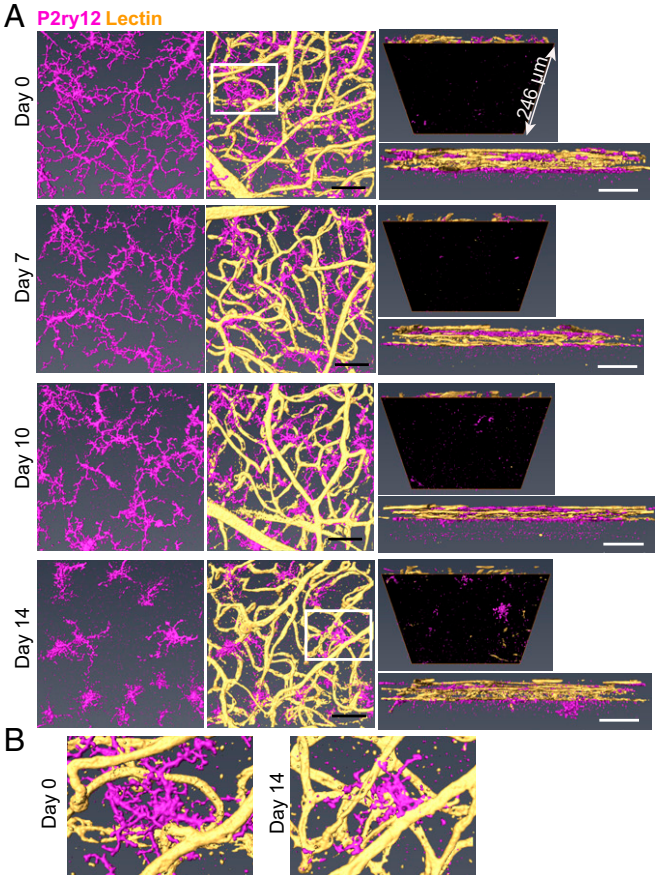

Fig. 6. Microglia interact with retinal vessels during development of EAU. EAU was induced in C57BL/6 mice, and whole-mount retinas were then stained with anti-P2ry12 antibody (magenta) and lectin (yellow) at 0, 7, 10, and 14 d after EAU induction. Confocal z-stack images of the entire retinal thickness in the midperipheral retina were taken and 3D-reconstructed using Amira software. (*A*) Representative images from a single scan area at each time point are shown: the top view of microglia (*Left*), the top view of microglia and lectin (*Center*), the bottom view (*Top Right*), and the side view (*Bottom Right*). The bottom view illustrates changes occurring under the retinal vascular bed (i.e., the outer nuclear layer and the photoreceptors), which are highlighted by masking the upper retina with an inserted black surface. (*B*) Magnified images of microglia from the areas surrounded by white squares in the images of day 0 and day 14 in *A*. At least four eyes were examined for each time point. (Scale bars: 50 μm.)

We next determined if microglia have direct contact with adherent leukocytes in the early phase of EAU. EAU was induced in C57BL/6 mice on a regular diet, and the retinas were collected for immunohistochemistry on days 7 and 10, which is when immune cells begin to infiltrate the retina in EAU. Antibodies against MHC class II, CD11b, or CD4/CD8 were used to label leukocytes, with labeling of microglia and blood vessels using P2ry12 and lectin, respectively. Under direct observation with confocal microscopy, microglia located close to intravessel leukocytes were chosen, and z-stack images of those microglia were taken. We observed direct association of microglia and adherent leukocytes through microglial processes using the z-stack and 3D-constructed images (Fig. 7 *C*–*E* and Movies S1–S8). Activated microglia are known to express MHC class II; however, we observed that morphologically activated microglia on day 7 (*SI Appendix*, Fig. S5 *A* and *B*) and day 10 (Fig. 7*C* and *SI Appendix*, Fig. S5*C*) were MHC class II$^-$. We identified an MHC-class II$^+$ adherent leukocyte population that interacts with microglia on day 7 of EAU (*SI Appendix*, Fig. S5*A* and Movies S1 and S2) and prominently on day 10 (Fig. 7*C* and Movies S3 and S4). Intravascular CD11b$^+$ cells and CD4/CD8$^+$ cells also directly interacted with microglia (Fig. 7 *D* and *E* and Movies S5–S8). The 3D-constructed images demonstrated that microglia have direct contact with these leukocytes (Movies S1, S3, S5, and S7), which are located on the intravascular wall (Movies S2, S4, S6, and S8). These adherent cellular populations have been implicated in EAU disease pathology; therefore, based on these observations, we suggest that microglia play a critical role in induction of EAU by directing the recruitment of leukocytes into the retinal microenvironment and likely trigger subsequent wide-scale inflammatory cell entry into the neuroretina.

Discussion

In this study, we used a Csf1r antagonist (PLX5622) known to eliminate microglia to determine the contribution of retinal microglia in the development of autoimmune uveitis induced by systemic immunization with IRBP. Our data indicate retinal microglia are essential for initiating infiltration of inflammatory cells during the early stages of EAU. In the absence of microglia, we did not detect evidence of either retinal infiltrating cells or inflammation, even when the mice possessed circulating primed IRBP-reactive immune cells that were shown to be fully capable of inducing EAU (Fig. 4 *B* and *C*). These data imply that monocytes/macrophages cannot replace the function of microglia, and trigger the development of EAU by initiating the infiltration of IRBP-reactive immune cells. Although Csf1r is also expressed on systemic monocytes/macrophages, treatment with PLX5622 did not affect the ability of mice to generate systemic IRBP-specific immune responses (Fig. 2 *A*–*E*). The EAU-inducing capability of autoreactive immune cells, using adoptive transfer experiments, indicated that systemic IRBP-specific immune cells were equally developed in PLX5622-treated and control-treated IRBP-immunized mice (Fig. 4*E*). Therefore, our data indicate the primary function of retinal microglia in autoimmune uveitis is to initiate disease and without microglia, no local inflammation will develop.

Our imaging studies further indicated that in IRBP-immunized mice, retinal microglia developed an activated morphology and became closely associated with retinal vessels before any evidence of uveitis (Fig. 6 and *SI Appendix*, Fig. S4). Moreover, these microglia had direct contact with a variety of adherent leukocytes in the retinal vasculature during the early phase of EAU (days 7–10), interacting not only with T cells but also with MHC class II$^+$ cells and CD11b$^+$ cells (Fig. 7 *C*–*E* and *SI Appendix*, Fig. S5 and Movies S1–S8). This observation suggests microglia have a direct effect on

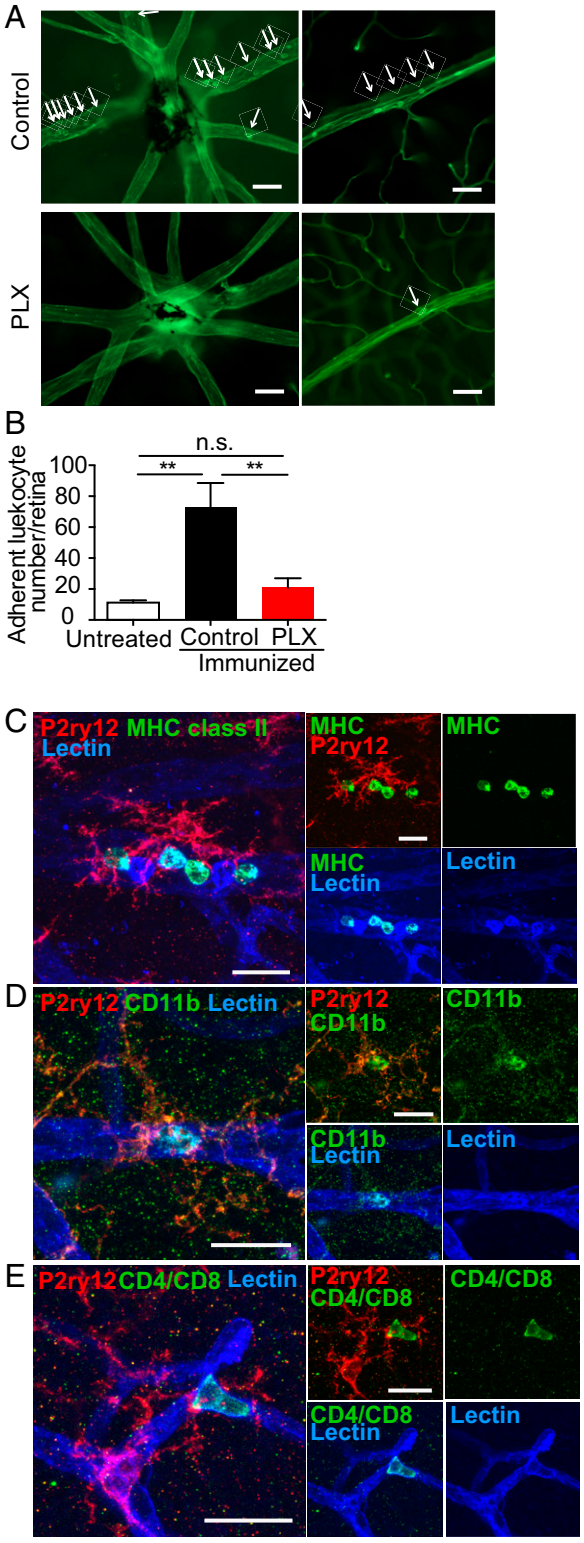

Fig. 7. Microglia interact with adherent leukocytes in the retinal vessels during the development of EAU. (*A* and *B*) EAU was induced in mice with or without microglia depletion by PLX5622 (PLX). On day 10, retinal adherent leukocytes were imaged by perfusion labeling with FITC Con A lectin. (*A*) Representative images of flat-mounted retinas from each group are presented. Images are shown around the optic disk (*Top*) and the midperiphery (*Bottom*). Adherent leukocytes are indicated by arrows. (*B*) Mean number of adherent retinal leukocytes in major vessels per eye. (n = 6–8 retinas per group). Data were analyzed by one-way ANOVA, followed by Tukey's multiple comparison test, and are expressed as mean ± SEM. $^{**}P < 0.01$. n.s., not significant. (*C*–*E*) EAU was induced in C57BL/6 mice, and retinas were collected on day 10. Whole-mount immunohistochemistry was performed using antibodies against MHC class II (*C*), CD11b (*D*), or CD4/CD8 (*E*) (all green), with P2ry12 (red) and lectin (blue) staining. Stained retinas were observed using confocal microscopy. Images of microglia that appeared to interact with adherent leukocytes were taken by confocal microscopy, and z-stack images were created using ImageJ (NIH). Representative images were obtained by observation of at least three retinas per group. (Scale bars: *A*, 50 μm; *C*–*E*, 20 μm.)

adherent vascular leukocytes, and supports our data that they regulate infiltration of circulating cells into the neuroretina.

Activated microglia are thought to function as local APCs, along with perivascular macrophages (37, 38), as microglia can express MHC class II upon activation; however, they do not express MHC class II under normal conditions (39, 40). Previous studies indicated that local APCs process and present retinal autoantigens that reactivate antigen-specific T cells once they infiltrate into the retina (41, 42), and it is these reactivated T cells that drive the development of retinal inflammation. Studies of APCs in EAU demonstrated that MHC class II expression is up-regulated in the retina during late stages of EAU (39, 43). However, MHC class II expression within the retina during the early phase of EAU is less clear, and the dominant APC population at this stage of disease has not yet been confirmed.

An unexpected result from our experiments was that immunohistochemical analysis of retinal whole mounts revealed that microglia interacting with adherent leukocytes in the early phase of EAU (days 7–10) were MHC class II^- (Fig. 7*C* and *SI Appendix*, Fig. S5), suggesting microglia at this early stage are not functioning as APCs. There are at least two possible explanations for these results. First, the retinal microglia we examined are, in fact, MHC class II^+, but the level of expression is extremely low and below the level of antibody detection. Arguing against this is our ability to detect MHC class II^+ APCs in the retinal vasculature in close proximity to microglia, indicating the sensitivity of our detection method is sufficient to identify MHC class II^+ APCs. The alternative explanation is that these microglia are MHC class II^- and, at this early phase of EAU, are not capable of antigen presentation to $CD4^+$ T cells. Since our data clearly indicate these microglia are responsible for triggering leukocyte infiltration into the retina, this suggests the microglia-mediated infiltration of inflammatory cells is antigen-nonspecific, and not mediated by MHC class II presentation of retinal autoantigens. Considering that microglia interact not only with T cells but also with MHC class II^+ cells and $CD11b^+$ cells, it seems that microglia could introduce a variety of cell populations into the retina. We speculate that IRBP-specific T cells and the matching MHC class II^+ cells are both randomly introduced into the retina with the support of microglia. This hypothesis may be supported by previous reports finding that early infiltration of leukocytes into the retina and the brain was observed in both antigen-specific and non–antigen-specific T cell transfer (41, 42, 44).

Our data seem to contradict the idea that under normal conditions, microglia are thought not to have access to circulating leukocytes and are physically separated from the blood stream by the endothelium that forms the blood-retinal barrier (29). However, microglia are part of the neurovascular unit surrounding the retinal vessels (45–48), together with endothelial cells, nerve endings, astrocytes, and pericytes. In this perivascular location, microglia likely survey the influx of blood-borne components entering the central nervous system. In diseased conditions, it is suggested that endothelium–microglia interactions contribute to a variety of inflammation-related pathologies in the brain, and that activated microglia could lead to the disruption of the blood–brain barrier (49, 50). It is also possible that cross-talk between microglia and astrocytes promotes blood–brain barrier

breakdown, as suggested in a recent report that inflammatory factors produced by LPS-activated microglia induced astrocyte activation (51).

Together, our data suggest that in the earliest stages of EAU, when circulating immune cells first begin to migrate into the retina, microglia function by an antigen-nonspecific mechanism to trigger vascular cell adherence and extravasation. This would result in leukocyte infiltration into the retina of a variety of cells, including antigen-specific T cells and MHC class II^+ cells. These infiltrating APCs could then reprocess and present retinal autoantigens, such as IRBP in this EAU model, that reactivate surrounding antigen-specific $CD4^+$ T cells. The reactivated $CD4^+$ T cells produce inflammatory cytokines that trigger local inflammation and blood-retinal barrier breakdown. This initial inflammation would be further amplified by promoting increased infiltration of systemic leukocytes, resulting in clinically apparent EAU (28, 29). Indeed, it has been suggested that EAU is initiated by local infiltrating dendritic APCs, and not by resident APCs (52). While retinal microglia may become MHC class II^+ in the later phases of EAU, they do not appear to be required to amplify and sustain inflammation, since depleting microglia after retinal inflammation had already started had no effect on the severity or duration of retinal inflammation. This indicates the primary function of retinal microglia is to trigger infiltration of circulating cells, while the amplification of antigen-specific autoimmunity is mediated primarily by infiltrating APCs.

The mechanism by which microglia detect very early systemic alterations in IRBP- immunized mice and become activated requires further elucidation. Microglial activation is apparent 7 d postimmunization (*SI Appendix*, Fig. S4), when there are no obvious leukocytes infiltrating into the retina. Therefore, it is likely that microglia detect very early changes occurring in the retina and the blood vessels, which may be induced by inflammatory factors produced by a small number of antigen-specific T cells that entered the retina early on. Since microglial processes are closely associated with retinal blood vessels even under normal conditions, it is possible that microglia interact with circulating immune cells independent of activation. In fact, recent reports revealed that microglia express various genes encoding surface receptors and molecules, for sensing endogenous ligands and microbes, that constitute a so-called "sensome." Given that sensome expression patterns are affected by sex and microbiome (53, 54), this might explain the differences in disease susceptibility between sexes and individuals. Although various inflammatory factors, such as ATP, IFN-γ, IL-17, VEGF, and GM-CSF (55–57), up-regulated in EAU have been shown to induce microglial activation (40, 58–61), the exact sequence of events leading to the initial activation of microglia remains incompletely understood, and is of significant interest.

In summary, we clearly demonstrated that microglial depletion blocks the induction of EAU by preventing the infiltration of circulating primed inflammatory cells, indicating the primary function of microglia is to trigger the infiltration of circulating leukocytes early in the development of disease. Although systemic exposure to an autoantigen is the trigger of autoimmunity in EAU, our results indicate microglia are the critical cell population in the retina that allows the entry of autoreactive cells required for the initiation of EAU.

Materials and Methods

Animals and Reagents. Female animals were used for all of the experiments. All animal experiments followed the guidelines of the Association for Research in Vision and Ophthalmology Statement for the Use of Animals in Ophthalmic and Vision Research and were approved by the Animal Care Committee of the Massachusetts Eye and Ear Infirmary. C57BL/6J mice (stock no. 00664), *Cx3cr1*^{CreER} mice (stock no. 021160), and B6-iDTR mice (stock no. 007900) were purchased from The Jackson Laboratory. Standard laboratory chow was fed to mice, except during the microglia depletion experiments, where PLX5622 or control diet was given. Mice were allowed free access to food and water in a climate-controlled room with a 12-h light/12-h dark cycle. All mice used for experiments were 7–9 wk of age. For anesthesia, i.p. injection of 250 mg/kg of 2,2,2-tribromoethanol (Sigma–Aldrich) was used for survival procedures, and 400 mg/kg was used for nonsurvival procedures. High-performance liquid chromatography–purified human IRBP-p was purchased from Biomatik. Complete Freund's adjuvant and *Mycobacterium tuberculosis* H37Ra were purchased from Difco. Purified *Bordetella* pertussis toxin, phorbol 12-myristate 13-acetate, ionomycin, Histopaque 1083, penicillin, and streptomycin were purchased from Sigma–Aldrich.

Induction of EAU. For active induction of EAU, 200 μg of IRBP-p was emulsified in complete Freund's adjuvant (1:1 wt/vol) containing an additional 5 mg/mL *M. tuberculosis* H37Ra. On day 0, 200 μL of the emulsion was injected s.c. in the neck (100 μL), one footpad (50 μL), and the contralateral inguinal region (50 μL). Concurrent with immunization, 1 μg of pertussis toxin was injected i.p.

Adoptive transfer EAU was induced as previously described (62), with minor modifications. Briefly, donor mice were immunized as described above, and at 14 d after immunization, the spleens and draining LNs were collected. Lymphocytes from spleens and draining LNs were cultured in the presence of 10 μg/mL IRBP-p and 10 ng/mL IL-23 (R&D Systems) for 72 h in RPMI 1640 supplemented with 10% FBS (Gibco), 2 mM glutamine (Gibco), 100 U/mL penicillin, and 100 μg/mL streptomycin. The nonadherent cells in suspension were transferred to new dishes on days 1 and 2 of culture. After 3 d, activated lymphocytes were purified by gradient centrifugation on Histopaque 1083 and counted. The cells were injected i.p. in 0.2 mL of PBS into recipient mice (5×10^7 cells per mouse).

Assessment of EAU. Fundus images were observed using a Micron IV retinal imaging microscope (Phoenix), and the clinical score of active inflammation was graded in a blinded manner on a scale between 0 and 4 in half-point increments as described previously (24), with brief modification. Briefly, trace chorioretinal lesions and minimal vasculitis were scored as 0.5. Mild vasculitis with small focal chorioretinal lesions (≤5) were scored as 1. Severe vasculitis with multiple chorioretinal lesions (>5) were scored as 2. A pattern of a linear chorioretinal lesion, subretinal neovascularization, and hemorrhage were scored as 3. Inflammation with large retinal detachment and severe hemorrhages were scored as 4. For histological assessment, enucleated eyes were fixed in a buffer of 70% methanol and 30% acetic acid. The fixed tissues were embedded in paraffin and processed. Sections of 5 μm were cut and stained with H&E. The severity of EAU in each eye was scored on a scale between 0 and 4 in half-point increments in a blinded manner, according to a semiquantitative system described previously (25). Briefly, focal nongranulomatous, monocytic infiltration in the choroid, ciliary body, and retina was scored as 0.5. Retinal perivascular infiltration and monocytic infiltration in the vitreous were scored as 1. Granuloma formation in the uvea and retina and the presence of occluded retinal vasculitis, along with photoreceptor folds, serous retinal detachment, and loss of photoreceptor, were scored as 2. In addition, the formation of granulomas at the level of the retinal pigment epithelium and the development of subretinal neovascularization were scored as 3 and 4 according to the number and the size of the lesions (63). The average of scores from both eyes was determined as the score of the animal.

Microglia Depletion. Microglia depletion was performed using *Cx3cr1*^{CreER} × B6-iDTR transgenic mice or chow containing the Csf1r antagonist PLX5622 (Plexxikon, Inc.). To generate transgenic mice, *Cx3cr1*^{CreER} mice, which express Cre-ER fusion protein from endogenous CX3CR1 promoter-enhanced elements, were crossed with B6-iDTR mice, which contain a flox-STOP-flox DTR in the ROSA26 locus. In this transgenic mouse system, Cre recombinase activation under control of the *Cx3cr1* promoter can be induced by tamoxifen, which leads to surface expression of DTR on CX3CR1-expressing cells. The activation of Cre recombinase was induced by five consecutive days of tamoxifen administration via eye drops (10 μL per drop of 5 mg/mL in corn oil) three times per day (22) in 6-wk-old mice. DTX (Sigma–Aldrich) was then administered in the anterior chamber (25 ng in 1 μL of saline) to deplete CX3CR1-expressing cells (23). Control mice were administered saline in the anterior chamber. For microglia depletion using PLX5622, mice were fed control chow (AIN-76) or chow containing 1,200 ppm of the Csf1r inhibitor PLX5622 1 wk before EAU induction. No obvious behavioral or health problems were observed as a result of the PLX5622-supplemented diet.

Immunohistochemistry of Whole-Mount Retinas. Anesthetized mice were perfused with 20 mL of PBS. Eyes were enucleated and fixed in 4% paraformaldehyde in 2× PBS for 15 min and then transferred to 2× PBS on ice for 10 min. After dissecting eyes, retinal whole mounts were prepared. Retinas were then transferred to ice-cold methanol and kept at −80 °C until use.

For immunohistochemistry, retinas were first blocked in a blocking buffer (0.3% Triton, 0.2% BSA, and 5% goat serum in PBS) for 1 h at room temperature and incubated with primary antibodies and Alexa Fluor 647-conjugated isolectin GS-B4 (1:100; Thermo Fisher Scientific) overnight at 4 °C. After washing, retinas were incubated with secondary antibodies for 4 h at 4 °C. Retinas were mounted after washing. Rabbit anti-P2ry12 antibody (1:500; a gift from H. Weiner, Brigham and Women's Hospital), rat anti-CD11b antibody (1:100, clone M1/70; Abcam), rat anti-MHC class II (1:1,000, I-A/I-E; BD Pharmingen), rat anti-CD4 (1:200, RM4-5; BD Pharmingen), and rat anti-CD8a (1:200, 53-6.7; BD Pharmingen) were used for primary antibodies. Alexa Fluor 594-conjugated goat anti-rabbit antibody, and Alexa Fluor 488-conjugated goat anti-rat antibody (1:500; Thermo Fisher Scientific) were used for secondary antibodies.

Delayed Hypersensitivity Measurement. Antigen-specific delayed hypersensitivity was measured as previously described (64). On day 19 after immunization, mice were injected intradermally with 10 μg per 10 μL of IRBP-p suspended in PBS into the pinna of one ear. Ear swelling was measured after 48 h using a micrometer (Mitutoyo). Delayed hypersensitivity was measured as the difference in ear thickness before and after challenge. Results were expressed as specific ear swelling (48-h measurement − 0-h measurement) for a test ear − (48-h measurement − 0-h measurement) for a control ear.

Flow Cytometric Analysis of LNs and Spleens. Cervical, axillary, and inguinal LNs and spleens (SPs) were harvested from naive mice and EAU mice fed with PLX5622 or a control diet. Single-cell suspensions (1×10^6 cells per sample) were blocked with anti-mouse CD16/32 monoclonal antibody (eBioscience) and stained with cell surface antibodies. Dead cells were stained with a LIVE/DEAD fixable dead cell stain kit (blue or violet) (Thermo Fisher Scientific). The following anti-mouse antibodies were used for staining: CD4-FITC (clone: GK1.5), CD25-phycoerythrin (PE) (PC61.5), Foxp3-PE-Cy7 (FJK-6s), CD11c-FITC (N418), CD11b-PE (M1/70), CD45-allophycocyanine (30-F11), IFN-γ–PE (XMG1.2), and IL-17A–allophycocyanine (eBio17B7) (all from eBioscience). CD3-Pacific blue (17A2) was purchase from BioLegend. For CD45/CD11b/CD11c detection, cells were subjected for analysis without fixation. For regulatory T cell (CD3/CD4/CD25/Foxp3) staining, after staining with cell surface markers, cells were fixed and permeabilized with a Foxp3 staining buffer kit (eBioscience) and stained with Foxp3-PE-Cy7. For Th1 and Th17 detection (CD3/CD4/IFN-γ/IL-17), single-cell suspensions were stimulated for 4 h with 50 ng/mL phorbol myristate acetate and 500 ng/mL ionomycin in culture media (10% FBS, RPMI 1640, penicillin, streptomycin, β-mercaptoethanol) in the presence of GolgiPlug (BD Biosciences). The cells were stained with CD3-pacific blue, CD4-FITC, and LIVE/DEAD blue, and then fixed and permeabilized using an intracellular fixation and permeabilization buffer set (eBioscience). The cells were next stained with IFN-γ–PE and IL-17–allophycocyanine. Flow cytometric data were acquired on an LSR II (BD Biosciences). Acquired data were analyzed using FlowJo version 10.1.

Lymphocyte Proliferation Assay. Draining LNs and spleens were collected, and cells were suspended at 2×10^5 cells per 200 μL of medium in 96-well, flat-bottomed plates. Cells were cultured in triplicate in the presence of 10 μg/mL IRBP-p, 1 μg/mL Con A (Sigma–Aldrich), or medium alone. During the last 4 h of the 72-h culture, 100 μL of supernatant in the culture medium was removed, 10 μL of Cell Counting Kit-8 (Sigma–Aldrich) was added to each well, and the cells were incubated for 4 h. At the experimental end point, the number of viable cells in each well was measured as the absorbance (450 nm) of reduced WST-8 (65).

Lectin Labeling of Adherent Retinal Leukocytes. The retinal vasculature and adherent leukocytes were imaged by perfusion labeling with FITC-conjugated Con A lectin (Vector Laboratories), as described previously, with modifications (66, 67). Briefly, after deep anesthesia, the chest cavity was opened and a 27-gauge cannula was inserted into the left ventricle. Mice were then perfused through the left ventricle first using 5 mL of PBS, followed by fixation with 1% paraformaldehyde (5 mL), 5 mL of FITC-conjugated Con A (20 μg/mL in PBS), and 5 mL of PBS. The eyes were then fixed in 4% paraformaldehyde for 15 min, and the retinas were flat-mounted. The total number of Con A-stained adherent leukocytes in the major retinal vessels (venules, arterioles, and collecting vessels) was counted under direct observation with an epifluorescent microscope (Axio Observer Z1; Carl Zeiss).

Image Processing and Analysis. The images of whole-mount retinas were captured using confocal microscopy (SP5 or SP8; Leica) or an epifluorescent microscope (Axio Observer Z1). To quantify the number of microglia, microglial cell bodies were manually counted based on the z-stack images. For microglial density evaluation, maximum intensity z-stack images were created, and images were processed with the smooth, make binary, and watershed tools. The area of particles was then calculated using the analyze particles tool, setting the size range to 5–1,000 μm^2. Amira five software (FEI) was utilized to develop 3D reconstructed images.

Quantification and Statistical Analysis. Data are presented as the mean ± SEM. Differences between two groups were analyzed using an unpaired *t* test or Mann–Whitney *U* test. Multiple-group comparison was performed by one-way ANOVA, followed by Tukey's or Dunnett's multiple comparison test. All statistical analyses were performed using graphing software (Prism 6; GraphPad Software, Inc.). Significance levels are marked as follows in the figures: $*P < 0.05$, $**P < 0.01$, $***P < 0.001$, and $****P < 0.0001$.

ACKNOWLEDGMENTS. We thank Plexxikon, Inc. for providing PLX5622 chow. Special thanks go to the Department of Ophthalmology (Harvard University) and Massachusetts Eye and Ear Infirmary for supporting this research. This study was supported by Grant R01EY027303 from the NIH/National Eye Institute, the Massachusetts Lions Eye Research Fund, and by an American Macular Degeneration Foundation Prevention Award (to K.M.C.).

1. Goto H, et al. (2007) Epidemiological survey of intraocular inflammation in Japan. *Jpn J Ophthalmol* 51:41–44.
2. Durrani OM, et al. (2004) Degree, duration, and causes of visual loss in uveitis. *Br J Ophthalmol* 88:1159–1162.
3. Lee RW, et al. (2014) Autoimmune and autoinflammatory mechanisms in uveitis. *Semin Immunopathol* 36:581–594.
4. Caspi RR, et al. (2008) Mouse models of experimental autoimmune uveitis. *Ophthalmic Res* 40:169–174.
5. Rizzo LV, et al. (1996) Establishment and characterization of a murine CD4+ T cell line and clone that induce experimental autoimmune uveoretinitis in B10.A mice. *J Immunol* 156:1654–1660.
6. Sanui H, et al. (1989) Identification of an immunodominant and highly immunopathogenic determinant in the retinal interphotoreceptor retinoid-binding protein (IRBP). *J Exp Med* 169:1947–1960.
7. Crane IJ, Liversidge J (2008) Mechanisms of leukocyte migration across the blood-retina barrier. *Semin Immunopathol* 30:165–177.
8. Ginhoux F, et al. (2010) Fate mapping analysis reveals that adult microglia derive from primitive macrophages. *Science* 330:841–845.
9. Okunuki Y, et al. (2018) Microglia inhibit photoreceptor cell death and regulate immune cell infiltration in response to retinal detachment. *Proc Natl Acad Sci USA* 115:E6264–E6273.
10. Rathnasamy G, Foulds WS, Ling EA, Kaur C (2019) Retinal microglia–A key player in healthy and diseased retina. *Prog Neurobiol* 173:18–40.
11. Connor KM, et al. (2007) Increased dietary intake of omega-3-polyunsaturated fatty acids reduces pathological retinal angiogenesis. *Nat Med* 13:868–873.
12. Peng B, et al. (2014) Suppression of microglial activation is neuroprotective in a mouse model of human retinitis pigmentosa. *J Neurosci* 34:8139–8150.
13. Ma W, et al. (2019) Absence of TGFβ signaling in retinal microglia induces retinal degeneration and exacerbates choroidal neovascularization. *eLife* 8:e42049.
14. Dagkalis A, Wallace C, Hing B, Liversidge J, Crane IJ (2009) CX3CR1-deficiency is associated with increased severity of disease in experimental autoimmune uveitis. *Immunology* 128:25–33.
15. Aslanidis A, et al. (2015) Activated microglia/macrophage whey acidic protein (AMWAP) inhibits NFκB signaling and induces a neuroprotective phenotype in microglia. *J Neuroinflammation* 12:77.
16. Karlstetter M, et al. (2014) Translocator protein (18 kDa) (TSPO) is expressed in reactive retinal microglia and modulates microglial inflammation and phagocytosis. *J Neuroinflammation* 11:3.
17. Reyes NJ, O'Koren EG, Saban DR (2017) New insights into mononuclear phagocyte biology from the visual system. *Nat Rev Immunol* 17:322–332.
18. Butovsky O, et al. (2014) Identification of a unique TGF-β-dependent molecular and functional signature in microglia. *Nat Neurosci* 17:131–143.
19. Ebneter A, Kokona D, Jovanovic J, Zinkernagel MS (2017) Dramatic effect of oral CSF-1R kinase inhibitor on retinal microglia revealed by in vivo scanning laser ophthalmoscopy. *Transl Vis Sci Technol* 6:10.
20. Valdearcos M, et al. (2014) Microglia dictate the impact of saturated fat consumption on hypothalamic inflammation and neuronal function. *Cell Rep* 9:2124–2138.
21. Hilla AM, Diekmann H, Fischer D (2017) Microglia are irrelevant for neuronal degeneration and axon regeneration after acute injury. *J Neurosci* 37:6113–6124.
22. Boneva SK, et al. (2016) Cre recombinase expression or topical tamoxifen treatment do not affect retinal structure and function, neuronal vulnerability or glial reactivity in the mouse eye. *Neuroscience* 325:188–201.
23. McPherson SW, Heuss ND, Pierson MJ, Gregerson DS (2014) Retinal antigen-specific regulatory T cells protect against spontaneous and induced autoimmunity and require local dendritic cells. *J Neuroinflammation* 11:205.
24. Thurau SR, Chan CC, Nussenblatt RB, Caspi RR (1997) Oral tolerance in a murine model of relapsing experimental autoimmune uveoretinitis (EAU): Induction of protective tolerance in primed animals. *Clin Exp Immunol* 109:370–376.

25. Caspi RR, et al. (1988) A new model of autoimmune disease. Experimental autoimmune uveoretinitis induced in mice with two different retinal antigens. *J Immunol* 140:1490–1495.
26. Elmore MR, et al. (2014) Colony-stimulating factor 1 receptor signaling is necessary for microglia viability, unmasking a microglia progenitor cell in the adult brain. *Neuron* 82:380–397.
27. Liyanage SE, et al. (2016) Flow cytometric analysis of inflammatory and resident myeloid populations in mouse ocular inflammatory models. *Exp Eye Res* 151:160–170.
28. Chen P, Denniston AK, Hirani S, Hannes S, Nussenblatt RB (2015) Role of dendritic cell subsets in immunity and their contribution to noninfectious uveitis. *Surv Ophthalmol* 60:242–249.
29. Luger D, Caspi RR (2008) New perspectives on effector mechanisms in uveitis. *Semin Immunopathol* 30:135–143.
30. Sun M, et al. (2010) Contribution of CD4+CD25+ T cells to the regression phase of experimental autoimmune uveoretinitis. *Invest Ophthalmol Vis Sci* 51:383–389.
31. Caspi RR (2003) Experimental autoimmune uveoretinitis in the rat and mouse. *Curr Protoc Immunol* Chapter 15:Unit 15.16.
32. Agarwal RK, Caspi RR (2004) Rodent models of experimental autoimmune uveitis. *Methods Mol Med* 102:395–419.
33. Bebo BF, Jr, et al. (2009) Treatment with selective estrogen receptor modulators regulates myelin specific T-cells and suppresses experimental autoimmune encephalomyelitis. *Glia* 57:777–790.
34. de Kozak Y, et al. (2004) Intraocular injection of tamoxifen-loaded nanoparticles: A new treatment of experimental autoimmune uveoretinitis. *Eur J Immunol* 34: 3702–3712.
35. Kezic J, McMenamin PG (2010) The monocyte chemokine receptor CX3CR1 does not play a significant role in the pathogenesis of experimental autoimmune uveoretinitis. *Invest Ophthalmol Vis Sci* 51:5121–5127.
36. Chu CJ, et al. (2013) Assessment and in vivo scoring of murine experimental autoimmune uveoretinitis using optical coherence tomography. *PLoS One* 8:e63002.
37. Davies LC, Jenkins SJ, Allen JE, Taylor PR (2013) Tissue-resident macrophages. *Nat Immunol* 14:986–995.
38. Chinnery HR, McMenamin PG, Dando SJ (2017) Macrophage physiology in the eye. *Pflugers Arch* 469:501–515.
39. Lipski DA, et al. (2017) MHC class II expression and potential antigen-presenting cells in the retina during experimental autoimmune uveitis. *J Neuroinflammation* 14:136.
40. Zinkernagel MS, et al. (2013) Interferon γ-dependent migration of microglial cells in the retina after systemic cytomegalovirus infection. *Am J Pathol* 182:875–885.
41. Thurau SR, et al. (2004) The fate of autoreactive, GFP+ T cells in rat models of uveitis analyzed by intravital fluorescence microscopy and FACS. *Int Immunol* 16:1573–1582.
42. Prendergast RA, et al. (1998) T cell traffic and the inflammatory response in experimental autoimmune uveoretinitis. *Invest Ophthalmol Vis Sci* 39:754–762.
43. Xu H, Dawson R, Forrester JV, Liversidge J (2007) Identification of novel dendritic cell populations in normal mouse retina. *Invest Ophthalmol Vis Sci* 48:1701–1710.
44. Hickey WF, Hsu BL, Kimura H (1991) T-lymphocyte entry into the central nervous system. *J Neurosci Res* 28:254–260.
45. Zlokovic BV (2008) The blood-brain barrier in health and chronic neurodegenerative disorders. *Neuron* 57:178–201.
46. Iadecola C (2004) Neurovascular regulation in the normal brain and in Alzheimer's disease. *Nat Rev Neurosci* 5:347–360.
47. Gardner TW, Davila JR (2017) The neurovascular unit and the pathophysiologic basis of diabetic retinopathy. *Graefes Arch Clin Exp Ophthalmol* 255:1–6.
48. Metea MR, Newman EA (2007) Signalling within the neurovascular unit in the mammalian retina. *Exp Physiol* 92:635–640.
49. da Fonseca AC, et al. (2014) The impact of microglial activation on blood-brain barrier in brain diseases. *Front Cell Neurosci* 8:362.
50. Sumi N, et al. (2010) Lipopolysaccharide-activated microglia induce dysfunction of the blood-brain barrier in rat microvascular endothelial cells co-cultured with microglia. *Cell Mol Neurobiol* 30:247–253.
51. Liddelow SA, et al. (2017) Neurotoxic reactive astrocytes are induced by activated microglia. *Nature* 541:481–487.
52. Jiang HR, Lumsden L, Forrester JV (1999) Macrophages and dendritic cells in IRBP-induced experimental autoimmune uveoretinitis in B10RIII mice. *Invest Ophthalmol Vis Sci* 40:3177–3185.
53. Hickman SE, et al. (2013) The microglial sensome revealed by direct RNA sequencing. *Nat Neurosci* 16:1896–1905.
54. Thion MS, et al. (2018) Microbiome influences prenatal and adult microglia in a sex-specific manner. *Cell* 172:500–516.e16.
55. Vinores SA, et al. (1998) Increased vascular endothelial growth factor (VEGF) and transforming growth factor beta (TGFbeta) in experimental autoimmune uveoretinitis: Upregulation of VEGF without neovascularization. *J Neuroimmunol* 89:43–50.
56. Iwata D, et al. (2010) Prevention of experimental autoimmune uveoretinitis by blockade of osteopontin with small interfering RNA. *Exp Eye Res* 90:41–48.
57. Zhao R, Liang D, Sun D (2016) Blockade of extracellular ATP effect by oxidized ATP effectively mitigated induced mouse experimental autoimmune uveitis (EAU). *PLoS One* 11:e0155953.
58. Couturier A, et al. (2014) Anti-vascular endothelial growth factor acts on retinal microglia/macrophage activation in a rat model of ocular inflammation. *Mol Vis* 20: 908–920.
59. Zimmermann J, et al. (2018) IL-17A promotes granulocyte infiltration, myelin loss, microglia activation, and behavioral deficits during cuprizone-induced demyelination. *Mol Neurobiol* 55:946–957.
60. Ponomarev ED, Maresz K, Tan Y, Dittel BN (2007) CNS-derived interleukin-4 is essential for the regulation of autoimmune inflammation and induces a state of alternative activation in microglial cells. *J Neurosci* 27:10714–10721.
61. Davalos D, et al. (2005) ATP mediates rapid microglial response to local brain injury in vivo. *Nat Neurosci* 8:752–758.
62. Zhang L, et al. (2016) Complement anaphylatoxin receptors C3aR and C5aR are required in the pathogenesis of experimental autoimmune uveitis. *J Leukoc Biol* 99: 447–454.
63. Chan CC, et al. (1990) Pathology of experimental autoimmune uveoretinitis in mice. *J Autoimmun* 3:247–255.
64. Kezuka T, et al. (2004) Peritoneal exudate cells treated with calcitonin gene-related peptide suppress murine experimental autoimmune uveoretinitis via IL-10. *J Immunol* 173:1454–1462.
65. Itano N, et al. (2002) Abnormal accumulation of hyaluronan matrix diminishes contact inhibition of cell growth and promotes cell migration. *Proc Natl Acad Sci USA* 99: 3609–3614.
66. Joussen AM, et al. (2001) Leukocyte-mediated endothelial cell injury and death in the diabetic retina. *Am J Pathol* 158:147–152.
67. Okunuki Y, et al. (2009) Suppression of experimental autoimmune uveitis by angiotensin II type 1 receptor blocker telmisartan. *Invest Ophthalmol Vis Sci* 50:2255–2261.